Int. J. Electrochem. Sci., 11 **(2016)** 8779 – 8796, doi: 10.20964/2016.10.26

International Journal of
ELECTROCHEMICAL
SCIENCE
www.electrochemsci.org

Corrosion and 3D crack-propagation Behaviors in Reinforced Concrete Subjected to Bending Load in Simulated Marine Environment

Zuquan Jin[1,*], *Xia Zhao*[2,*], *Tiejun Zhao*[1], *Li Yang*[1]

[1] College of Civil Engineering, Qingdao Technological University, Qingdao, China
[2] Key laboratory of Marine Environmental Corrosion and Bio-fouling, Institute of Oceanology, Chinese Academy of Science, Qingdao, China
[*]E-mail: jinzuquan@126.com, zhxiakk@163.com

Received: 13 June 2016 / *Accepted:* 6 August 2016 / *Published:* 6 September 2016

The corrosion-cracking behavior of reinforced concrete subjected a sustained bending load and exposed to simulate marine environments was studied. The simulated marine environments include an atmosphere zone, a submerged zone and a tidal zone. The corrosive crack distribution in the inside of a concrete was observed using X-CT nondestructive technology. Results showed that the bending load caused both the corrosion rate of steel bar and the crack propagation inside the concrete to accelerate. These effects become apparent when the load exceeds50% of the ultimate load. The negative effect of the bending load on the accelerated corrosion rate of reinforced concrete in the submerged marine environment is even more significant than that in an indoor atmospheric environment. The constant potential accelerate test with embedded auxiliary stainless rebar electrode is not an appropriate accelerated choice to study the corrosion behavior of reinforced concrete in the submerged and tidal zones because the potential accelerates the chloride ion penetration into the concrete, and embedded auxiliary stainless rebar electrode changes the crack direction from the steel bar induced by corrosion.

Keywords: reinforced concrete; potentiostatic acceleration; bending load; X-CT; marine environment

1. INTRODUCTION

In marine environment, reinforced concrete is widely used as a construction material for infrastructures. However, the corrosion of steel bars induce by salinity is always considered a major threat to the safety of the structures. The deterioration of the steel bars due to corrosion has contributed to more than 80% of all the damages in reinforced concrete structures [1-3]. In past years, research had been conducted on ions transportation and evolution of concrete properties under simulated marine

environment and natural exposed environment [4-9]. In these severe environments, corrosion rates can exceed 500 μm/year[10].Besides salt water, corrosion is also affected by other factors, such as compactness of reinforced concrete, the homogeneity and thickness of the concrete cover, types of corrosion ions, environmental humidity and temperature [11-14].

For seaport wharf, reinforced concrete beam is simultaneously subjected to bending load and seawater. Hence, its corrosion rate is often higher than other parts of the structure[15]. Results by Li[16]and Bassuoni[17] showed that the external load altered the properties of the pore structure which can cause cracks to form in the cementitious matrix. These cracks enable chloride ions to penetrate which can lead to direct ingress of solution into considerable depth within the specimens. Jaffer[18] and Fang [19]found that the bond behavior was significantly weakened by the cyclic loading. The opening and closing of the cracks in salt solution under dynamic load forced the corrosion products to move from the rebar/concrete interface into the cracks. Further, both short-term and long-term experimental results by Hariche and Du [20-21]indicated that the maximum deflection and flexural capacity of a beam decreased with increasing applied load. Further, the corrosion of the reinforcement changed the failure mode from yielding followed by concrete crushing for the control beam to brittle failure of the corroded tension bars. While bending load can accelerate the chloride-induced corrosion rate of reinforced concrete, however, there are different corrosion characteristics for reinforced concrete that is exposed to different marine corrosion zones, such as the atmosphere zone, the submerged zone, and the tidal zone [22].This is because the key damage factors, such as electric conductivity, oxygen and chloride ion contents, humidity in corrosive cracked reinforced concrete, change in marine corrosion zone. Hence, there is an interactive effect between the bending load and the marine environment on the damage of reinforced concrete. The positive and negative effects of the bending load on corrosion of steel bar in concrete in different marine zones should be identified.

Under the natural conditions, the corrosion process of reinforced concrete is imperceptible and usually the initial signs of deterioration can be observed after many years of exposure. So, accelerated corrosion tests, including the constant current density and constant potential test, have been used to study the corrosion process of reinforced concrete [23-24]. However, the corrosion mechanism in reinforced concrete during the accelerated corrosion tests may not be the same as that under the natural conditions. This is because the degree of influence of the variables, such as oxygen and chloride ion contents, on the corrosion of reinforced concrete is different in the accelerated corrosion tests as compared to that in the natural conditions. Therefore, it is necessary to determine or measure some results to decide whether or not the accelerated corrosion tests are suitable for studying the corrosion process of reinforced concrete in marine environments.

Further, the stress distribution in the compressive zone and flexural zone of a reinforced concrete beam subjected to bending load is different, the corrosion and cracking processes in these zones are therefore also different. Based on an analysis of a 26-year-old corroded RC beam, Zhu[25] found that the corrosion cracks were more developed on the tensile surface, both in frequency and width. Goitseone[26-27]tested the longitudinal tensile strains and lateral deformation of RC beams under simultaneous loading and steel corrosion. The results showed that larger tensile strains were found on the surfaces of beams that were exposed to the corrosion environments whilst the side faces were mostly in compression prior to the cracking of the concrete cover. After the concrete cover was

cracked, larger and increasing tensile strains were measured on the cracked sides while the uncracked sides remained in compression. Longitudinal tensile strains of the corroded beams increased monotonically with time at a decreasing rate. However, these test results all came from the surface of the reinforced concrete. The corrosive crack actually originated from the inside of the reinforced concrete. Microscopic observation was used to look for the internal damage of the reinforced concrete specimens. However, prior to the observation, the specimens has to be cut, so this method was destructive [28, 24]. Nondestructive testing technology can detect in-situ damage point without destroying the structure. Recently, the gamma-ray radiography was successfully used to determine the depth of a pit[29]. Further, in recent years, X-CT technique has been developed as a nondestructive testing technology for concrete structures. It can receive 3D and 2D images and defect distribution on materials without any destruction and previous drying treatment to diagnosis the corrosive cracked reinforced concrete. Recently, it has also been applied to study the development of microstructure fracture, sulfate attack and carbonation of concrete[30-32].

In this study, the corrosive crack process of reinforced concrete under simultaneous bending load and simulated marine corrosion zones including the atmospheric zone, the submerged zone and the tidal zone has been carried out. The corrosive cracked reinforced concrete was observed using X-CT technique in-situ. The objectives of this study are to deepen the understanding of the corrosion mechanism of reinforced concrete caused by the coupled factors of bending load and marine environment, to assess the suitability of the constant potential corrosion test to accelerate the corrosion process in reinforced concrete in marine environments, as well as to provide a means for nondestructive observation of the corroded reinforced concrete. The results from this study are useful for corrosion control and service life prediction of reinforced concrete beams in the coastal area environment.

2. EXPERIMENTAL PROCEDURES

2.1. Materials and specimen preparation

P.I.52.5 Portland cement in accordance with Chinese standard GB175-2007, with a compressive strength of 59.8 MPa at the age of 28 days, was used in this study. Table 1 shows the chemical composition of cement.

Table 1. Chemical compositions of Portland cement

Constituent (wt%)	SiO_2	Al_2O_3	Fe_2O_3	CaO	MgO	TiO_2	Na_2O	K_2O	SO_3	Cl
Cement	21.8	5.42	3.44	66.01	1.26	0.36	0.57	0.33	0.66	0.00

The coarse aggregate was crushed granite with a maximum size of 25mm, and river sand with a fineness modulus of 2.6 was used as the fine aggregate. A polycarboxylicether-based superplasticizer

was used, and its dosage was adjusted to keep the slump of fresh concrete in the range of 140mmto 180 mm. The concrete mixtures were prepared with an effective water-to-cement ratio(w/c) of 0.33 and 450kg/m^3 binders. The mixture proportions for the reinforced concrete were 1:1.58:2.37:0.33 for cement: sand: aggregate: water, respectively, and the compressive strengths of the concrete cured for 7d and 28d were 36.5MPa and 63.9MPa, respectively.

The size of reinforced concrete specimen was 100mm×100mm×400mm. The longitudinal reinforcements consisted of three bars. The first one: carbon steel bar with 12 mm diameter deformed in the compressive zone; the second one: the specimen with a 25 mm effective cover in the flexural zone; the third one: stainless steel bar with 8 mm diameter in the middle of the concrete specimen. The carbon steel bar was cleaned and coated with cement paste followed by epoxy coating at the concrete-air interface. The surface of the deformed carbon steel bar was polished by 200# sand paper. The steel bars were degreased by acetone just before it was placed in the mold, and the effective exposure length of the steel bar was 360mm. Reinforced concrete samples were cast and placed at room temperature in the mold, which was subsequently removed after 48h. Finally, all specimens were cured under the condition of 20°C±3 °C and 95% relative humidity for 28d.

2.2 Accelerated corrosion of reinforced concrete under sustained bending load

The simultaneous load was applied to the specimens in four points bending, and it was sustained by steel frames with dual springs. The loading (as a fraction of the ultimate bending load of concrete) was 30% and 50%.

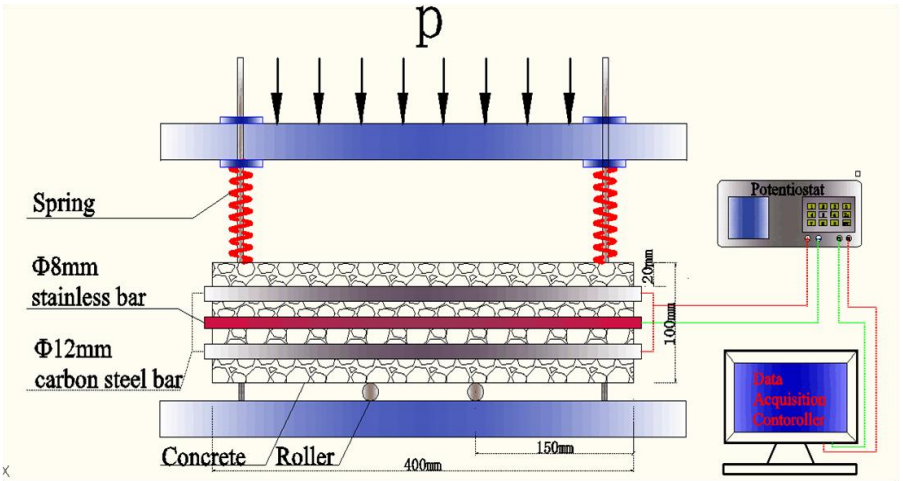

Figure 1. Potentiostatic accelerated corrosion of reinforced concrete under sustained bending load

The reinforced concrete under sustained bending load was exposed to three series of simulated environments: (1) the atmosphere zone, room environment with 75% relative humidity(RH) at 20°C±3 °C; (2) the marine submerged zone, concrete specimens immersed into tap water and seawater; (3) the marine tidal zone, concrete specimens were first dried at 40°C for 6h, and then immersed in seawater for 6h. The seawater was taken from Jiao Zhou Bay and the main chemical composites was (in wt. %) 1661 mg/l SO_4^{2-}, 17799 mg/l Cl^-, 1296mg/l Mg^{2+} with the pH =8.3. The reinforced concrete under

sustained bending load was subjected to accelerated corrosion current supplied by a potentiostatic through the carbon steel bar (connected to the positive electrode) and the embedded auxiliary stainless steel bar (connected to the negative electrode). Further, the electric potential was kept at a constant 30V, the current was checked every 2 h. Fig.1 shows a sketch and a photograph of the test setup.

2.3 X-CT measurement

After the accelerated corrosion test was completed, using a vacuum method, the samples with cracks were filled with epoxy and cured for three days. Then, specimen of 100mm×100mm×27mm were cut from the pure bending section of the concrete, which exposed to simulated submerged zone, and examined visually using X-CT system (YXLON, Civil engineering material key laboratory in Southeast University). A 3D image and the X, Y, Z scales of specimens are shown in Fig. 2. For the specimens, the X scale was from 10.22-36.92mm, the Y scale was from 6.44-103.68mm, and the Z scale was from 1.83-101.2mm. The voltage and current of the X-ray tube were 225 kV and 0.65 mA, respectively. The detector was the flat panel Y.XRD1620, which has1024detector elements. The number of projections was 1080. The size of the2D pixel was 0.14 mm × 0.14 mm, and the numbers of pixels were 1024 ×1024. The object rotation angles are 360 degrees. The resolution of X-CT system used in this test is 100μm.

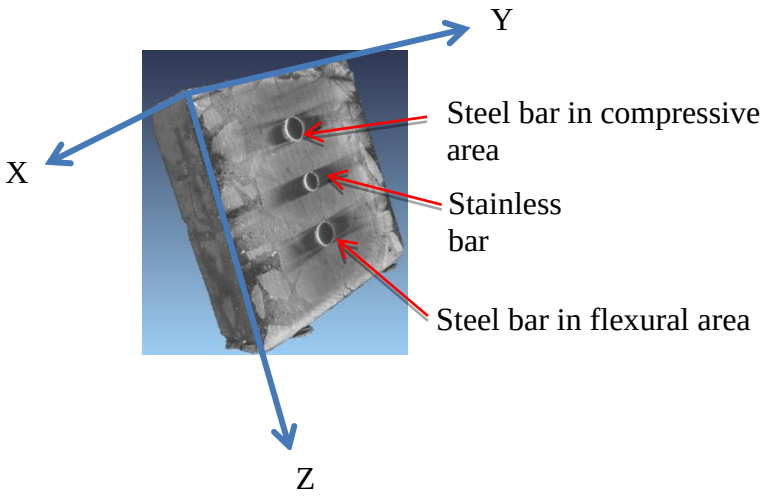

Figure 2. 3D image of specimen from the pure bending stress section of concrete corroded in seawater

3. RESULTS AND DISCUSSION

3.1 Simulated atmosphere zone

Concrete specimens under sustained bending load were polarized by a constant voltage of 30V. Fig. 3 shows the electric currents of the steel bar in the compressive zone and the flexural zone of the concrete. It can be seen that the electric current decreases faster during the early stage as compared to

that during the latter stage. The slower decrease in the electric current is because the concrete has cracked.

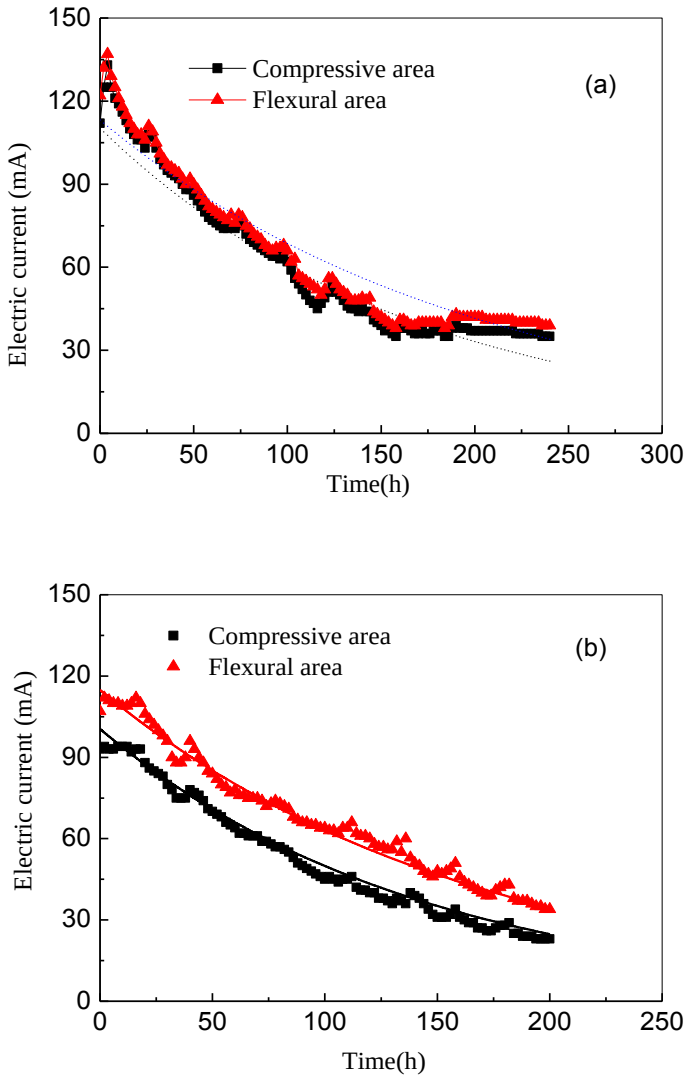

Figure 3. Electric current evolution of reinforced concrete under different bending loads. (a)30% load level, (b)50% load level

The theoretical amount of corrosion products is related to the electrical energy consumed, which is a function of voltage, amperage, and corrosion time interval. For a given electrolysis, the quantity of charge used can be calculated by the product of time and current. During the corrosion process, for every 1mol of iron is oxidized, there are 2 mols of electrons lost, consuming a charge of 2F, F is Faraday Constant with the value of 96487 C/mol. The mass loss(Δw) can be obtained from multiplying the quantity of charge by the molar mass (M) and dividing by the consuming charge needed for per mole[33], as shown in Eq.(1).

$$\Delta \mathrm{w} = \frac{t \times i \times M}{2F} \qquad (1)$$

Where, t is the corrosion time(s), i is the electric current of reinforced concrete(A), for iron, M is 55.847 g/mol.

By applying a regression model to the data as shown in Fig. 3, the relationship between electrical current and corrosion time is:

$$i_t = i_0 \times \exp(at) \quad (2)$$

Where, i_t is the electric current of reinforced concrete at time t (mA), i_0 is the electric current of reinforced concrete at the initial time (mA), and a is the regression coefficient.

According to Eqs.(1) and (2), the theoretical amount of corrosion products can be determined as follows:

$$\Delta w = \int_0^t \frac{i_0 \times \exp(-at) \times 10^{-3} \times 3600 \times M}{2F} dt \quad (3)$$

Put the value of M and F in Equation(3) and calculated, the following equation can be obtained:

$$\Delta w = \int_0^t 0.001042 \times i_0 \times \exp(-at) dt = \frac{1.042 \times 10^{-3} i_0}{a} (1 - \exp(-at)) \quad (4)$$

Further, because the corrosion rate is closely related to the amount of corrosion products, in this paper, the theoretical corrosion rate of steel bar in reinforced concrete was determined as follows:

$$\rho = \frac{\Delta w}{w_0} = \frac{\Delta w}{l \bullet m_0} = \frac{1.042 i_0 \times (1 - \exp(-at))}{a \times 890 \times 360} \quad (5)$$

Where ρ is theoretical corrosion rate of steel bar, w_0 is the initial mass of steel bar, which is the product of its length (l) and unit weight (m_0). In this study, the unit weight of the 12mm diameter deformed steel bar is 0.89mg/mm, and its exposure length is 360 mm.

When the reinforced concrete was subjected to 30% and 50% of the ultimate bending load, the times when the concrete first cracked (hereafter referred to the initial crack times)were recorded, and they were118 h and 112h, respectively. Fig. 4 shows the variation of the theoretical corrosion rate of steel bar in concrete subjected to 30% and 50% of the ultimate bending loads.

As shown in Fig.4, the corrosion rate of steel bar in the flexural zone is higher than that in the compressive zone. However, the difference is not apparent when the concrete had no cracks, especially when the concrete was subjected to 30% of the ultimate bending load. In the simulated atmosphere environment, the oxygen concentration and humidity are the key factors affecting the corrosion of steel bar in concrete. Because the concrete specimens were cured at 95% relative humidity for 28d and the potentiostatic accelerated corrosion was conducted at 75% RH only for 250h, the RH on the steel bar surface was almost saturated. Hence, the dominant factor for the corrosion of reinforced concrete in the atmosphere environment is the concentration of O_2 and not humidity. At the uncracked state, it can be seen from Fig.4 that there is little difference in the corrosion rate in the compressive zone and in the flexural zone, which indicates that the acceleration effect of small bending load level on O_2 migration into uncracked concrete is insignificant. In addition, higher loading will not increase the corrosion rate of reinforced bar in concrete in the atmospheric environment. Experimental results from R.R.Hussain [34] indicated that oxygen diffusion under normal dry air condition is not limited by external factors. The oxygen content will not be lack even the corrosion rate of steel bar increases. Therefore, the influence of bending load on oxygen diffusion into concrete is too small to be ignored. The bending load will not increase the corrosion rate of steel bar in uncracked concrete.

However, when the reinforced concrete has corrosive cracks, the impact of the bending loads on O_2 penetration increases gradually, and the trend increases with increasing bending load. So, the corrosion rate of steel bar changes accordingly. Fig. 5 shows the propagation of the corrosive crack in reinforced concrete subjected to 30% and 50% of the ultimate bending load in atmospheric environment. It is apparent that higher the bending load, the more rapid is the crack-propagation. Experimental results from Zhao[28] shown that after cracked, the outer solution can penetrate the concrete cover and ingress into the surface of the steel bar, then, some corrosion products dissolve in the solution and are carried away from the steel bar by the solution, and penetrate into the edges of cracks. The amounts of corrosion products and swelling stress would increase with the crack width, causing increment of crack propagation velocity. In addition, the exposed steel bar at the crack site can be regarded as anode, while the steel bar hid at the uncracked section is cathode. The greater crack width would lead to the expansion of anode area, improve the electrochemical reaction rate and the amount of the corrosion products, and ultimately increase the crack propagation velocity.

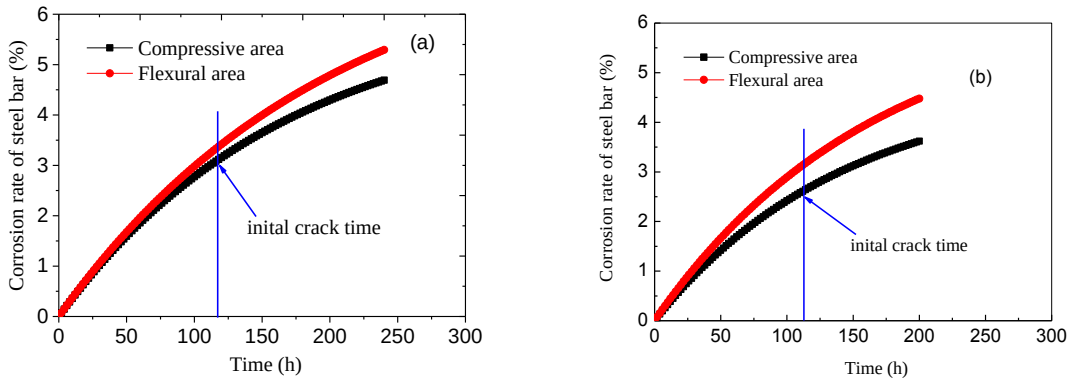

Figure 4. The theoretical corrosion rate of steel bar in concrete under different bending loads. (a) 30% load level; (b)50% load level

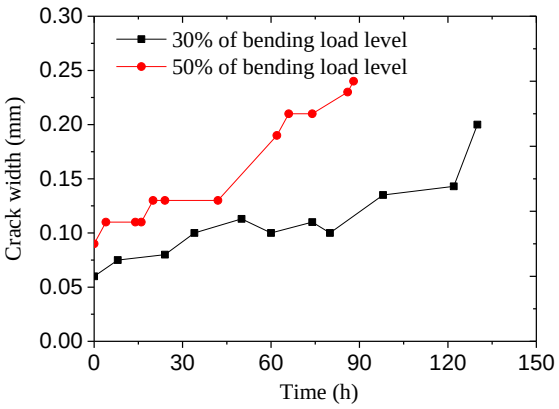

Figure 5. Corrosive crack propagation of reinforced concrete under bending load in atmospheric environment

3.2 Submerged environment

The variation of the electric current in reinforced concrete subjected to 50% of the ultimate bending load and immersed in tap water was tested and plotted in Fig.6. During the initial stage, the electric current increases because water was penetrating into the concrete thereby increasing the electric conduction. After that, the electric current decreases due to the generation of corrosion products. During the final stage, the electric current increases with time due to the direct ingress of water into the concrete through the cracks induced by the corrosion of the steel bars. The relationship between the electric current and time can be fitted by a simple quadratic function as follows:

$$i_t = m + n \times t + b \times t^2 \quad (6)$$

where i_t is the electric current in reinforced concrete at corrosion time t, and m, n, b are the regression coefficients.

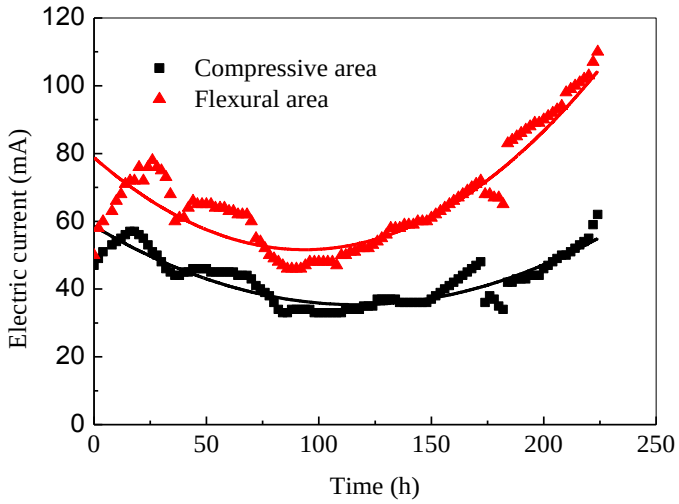

Figure 6. Electric current of steel bar in concrete under 50% bending load immersed into tap water

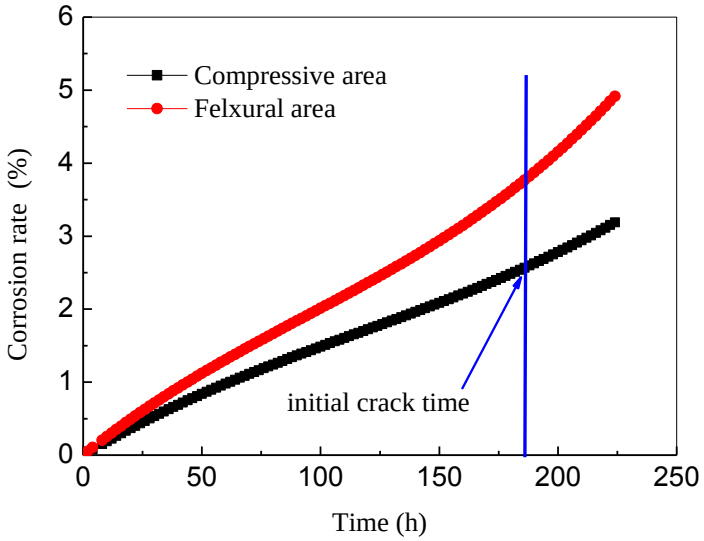

Figure 7. Corrosion rate of steel bar under 50% bending load immersed into tap water

Further, the theoretical corrosion rate of steel bar in reinforced concrete can be determined, as follows:

$$\rho = \frac{\Delta w}{w_0} = \frac{\int_0^t \frac{(m + n \times t + b \times t^2) \times 10^{-3} * 3600 * M}{2 \bullet F} dt}{l \bullet m_0} = \frac{\int_0^t 0.001042 \times (m + nt + bt^2) dt}{l \bullet m_0} = \frac{1.042 \times 10^{-3} \times (\frac{bt^3}{3} + \frac{nt^2}{2} + mt)}{l \bullet m_0} \quad (7)$$

Based on Eq.(7), Fig. 7 shows the theoretical corrosion rate of the reinforced concrete subjected to bending load and immersed in in tap water. It is apparent that the corrosion rate of steel bar in the flexural zone of concrete is higher than that in the compressive zone, and the trend is a gradual increase in corrosion rate with time.

The initial crack times of the reinforced concrete under bending load exposed to the atmosphere environment and the submerged environment are 112h and 184h, respectively. The delay of 72h in the submerged environment is due to the decrease of O_2 concentration. From Fig.4(b) and Fig.7, it can be seen that the corrosion rate of reinforced concrete in the atmosphere environment increases slowly after the concrete has cracked, but in the submerged environment, it increases quickly in the latter corrosion stage. Further, the negative impact of the bending load on the accelerated corrosion rate of the reinforced concrete in the submerged environment is more obviously than that in the atmospheric environment. This is related to the corrosion mechanism of steel bar in concrete under the constant potential accelerated test conditions. Apart the concentrations of oxygen, water and chloride ion, the corrosion rate of steel bar in concrete is affected by the resistance of concrete. The higher the resistance of concrete was, the more difficultly the charge could be transferred, and the slower the corrosion rate of steel bar would be. Since the corrosive cracks first appear on the flexural side of reinforced concrete under a bending load that is exposed to the submerged environment, water reaches the surface of steel bar in a very short period of time. The results in a decrease in resistance in the flexural zone and increases the corrosion rate of steel bar during latter period of corrosion. Meanwhile, the concrete cover on the compressive side of reinforced concrete is still uncracked even though the concrete cover on the flexural side is cracked. The corrosion rate of the steel bar in the flexural zone is higher than that in the compressive zone because of the difference in water content. So, the negative effect of bending load on the corrosion rate of steel bar becomes more apparent after the initial crack of concrete.

Fig. 8 shows the measured electric current in the reinforced concrete subjected to 30% and 50% of the ultimate bending load and immersed in seawater. Further, based on Eq.(7), the theoretical corrosion rate was calculated by Eq.(7) and shown in Fig.9. A comparison of Fig.6 and Fig.8 shows the variations of the electric current and the corrosion process is the same for the reinforced concrete submerged in tap water and seawater. However, the initial crack times of the reinforced concrete subjected to 30% and 50% of the ultimate bending load are only 70h and 40h, respectively. Fig. 10 shows the corrosive crack process in the flexural zone of concrete under bending load in seawater. It is apparent that the crack width in the concrete cover increases approximately linearly with time. Further, the higher bending load level causes a faster propagation of the cracks. As compared to the concrete in tap water, the chloride ion in seawater increases the corrosion rate of the steel bar and the crack propagation in concrete under bending load.

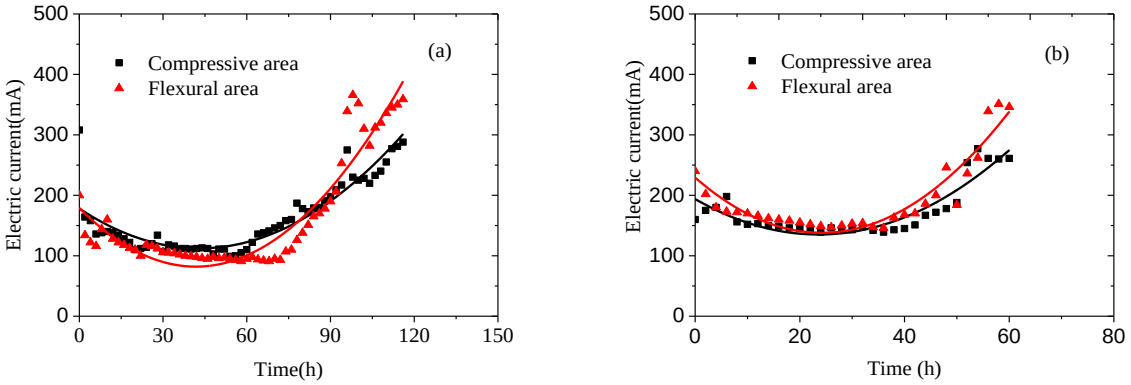

Figure 8. Electric current evolution of reinforced concrete under bending load. (a) 30% load level, (b) 50% load level

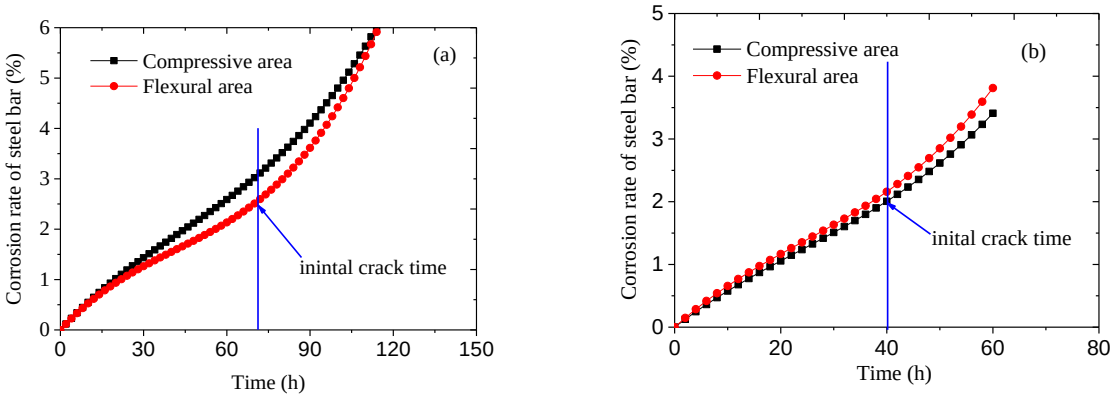

Figure 9. Corrosion rate of steel bar under different bending load in seawater. (a) 30% load level; (b)50% load level

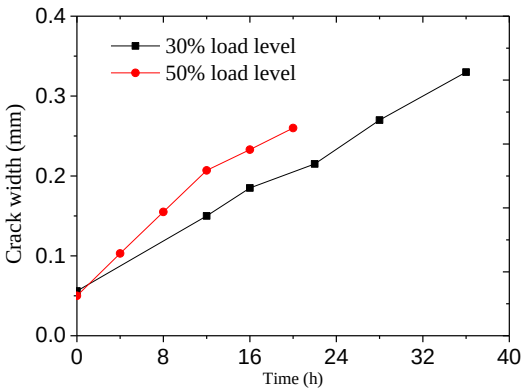

Figure 10. Corrosive crack propagation of reinforced concrete under bending load

The initial crack time of the reinforced concrete occurs earlier in Fig. 9 comparing to that in Fig.7, which is due to the presence of chloride ions. On the other hand, the negative impact of bending loads on the accelerated corrosion rate of steel bar in the flexural zone of the reinforced concrete decreases. This is because, in seawater, concentration of chloride ion is an important factor which causes corrosion of steel bar. Under the natural marine exposure condition, the tensile loading accelerates the penetration rate of chloride ions into the concrete, which causes the steel bar to corrode

faster. And experimental results from Lei[16] indicates that the external load could alter the pore structure properties within concrete and change the tensile stress in favor of chloride ion penetration. Fig.11 also shows the distribution of chloride ions in the concrete under the accelerated corrosion and the spontaneous conditions. It is apparent that under the constant potential accelerated corrosion conditions, the penetration of chloride ions is significantly higher than that under the natural condition, which results in a higher concentration of chloride ions on the steel bar surface and reaches its critical concentration within a short period of time. Therefore, under the constant potential acceleration, the negative effect of the load on the accelerated penetration of chloride ions will be reduced.

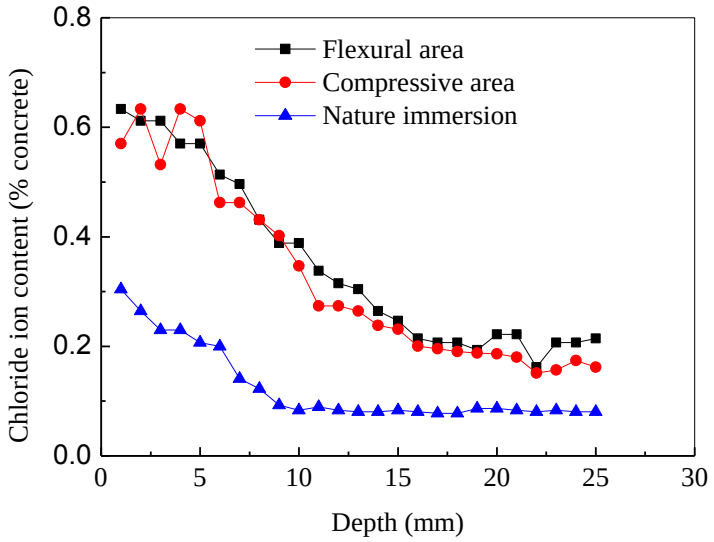

Figure 11. Chloride ion distribution in concrete under accelerated corrosion and spontaneous condition

Due to the little difference in chloride ions concentration in the flexural zone and in the compressive zone, the corrosion rate of the steel bar in these two zones are about the same, and the cracking times of the concrete are also about the same. After the concrete has cracked, the width and the density of cracks in the compressive zone are similar as that in the flexural zone. So, the effect of the flexural load is not significant.

3.3Tidal environment

Fig.12(a) shows the instant electric current in the reinforced concrete subjected to 50% of ultimate bending load and exposed to the simulated tidal environment. It is apparent that the variation in current is consistent with the tidal-type rule. The electric current increases during 6 hs wetting period, while decreases during 6 hs drying period. Using a linear interpolation method, the mean values of the rise and fall stage of each cycle were determined, and the overall evolution of the corrosion current was plotted as shown in Fig.12(b). It is apparent that the general trend is the same as that in the submerged environment, that is, the current decreases during the early stage and increases in the latter stage. Further, the current in the flexural zone is higher than that in the compressive zone.

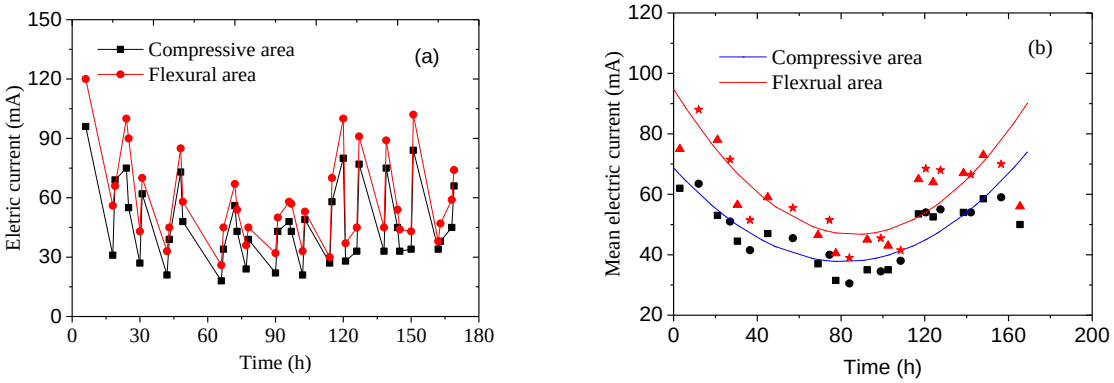

Figure 12. Electric current evolution of reinforced concrete under bending load exposed to tidal environment. (a) instant current; (b) mean current

According to the variation in the current, Eq.5 was used to calculate the theoretical corrosion rate of the steel bar in the reinforced concrete exposed to the tidal environment, which is shown in Fig.13. It is apparent that the trends of the corrosion rate are similar to those in the submerged environment, except for the smaller values. The initial crack time of the reinforced concrete in the tidal environment is 121h, which is longer than that in the submerged environment. This can be attributed to the variation in the resistance of concrete under the wet-dry cycles of the tidal environment, where the humidity of the concrete changes periodically. Further, the electrical conductivity of concrete is correlated with water content, which results in an increase or decrease in the resistance during the wet and dry cycles. Although the wet-dry cycles cause the acceleration in the penetration of chloride ions into concrete, the acceleration effect is weaker than that in the constant potential acceleration method. From Fig.11, it can be seen that the concentration of chloride ions in 25mm depth of concrete is about 0.2%, far higher than its critical value. Hence, the effect of chloride ions in concrete can be neglected under the wet-dry cycles in the constant potential acceleration method. However, during the drying period, the concrete resistance increases, the mean resistance under the wet-dry cycles is higher than that during the long-term immersion period, which causes the corrosion rate of steel bar under the wet-dry cycles to be lower than that during the long-term immersion period.

In real-life tidal environment, the tidal effect accelerates the penetration of chloride ion into concrete. The concentration of chloride ion therefore reaches the critical value earlier. Hence, the steel bars in the concrete corrode and crack earlier than those in the submerged environment. The corrosion rates of the steel bars in concrete that is within tidal and splash zones are higher than those under the long term immersion condition. Therefore, the law of chloride ion in concrete under the condition of marine environment is different from that in the constant potential acceleration method. The results from the accelerated corrosion test is inconsistent with that in real-life situations [15,22].

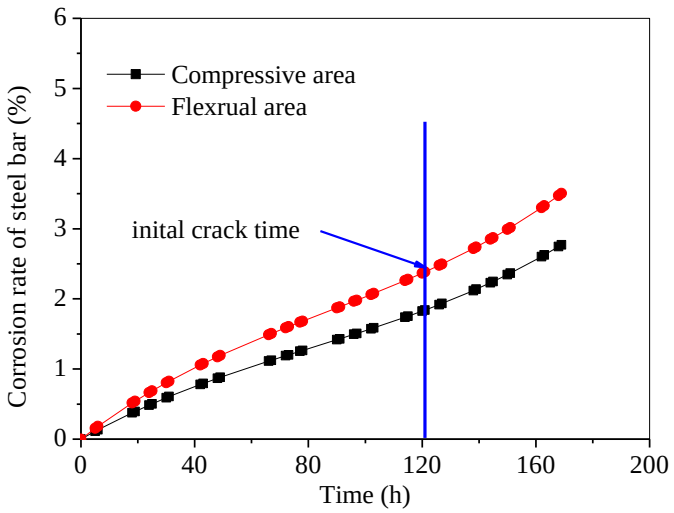

Figure 13. Theoretical corrosion rate of steel bar in tidal environment

3.4Corrosive crack observed by X-CT

The images of the concrete specimen on the YZ plane at various depths were shown in Fig.14. The aggregate, reinforced bar, and the crack distribution in the concrete are significantly different according to the gray scale of the images. The corrosive crack propagated throughout the specimen along with the position of steel bar. The concrete cover of the steel bar in the Y and Z directions are 44mm and 25mm, respectively.

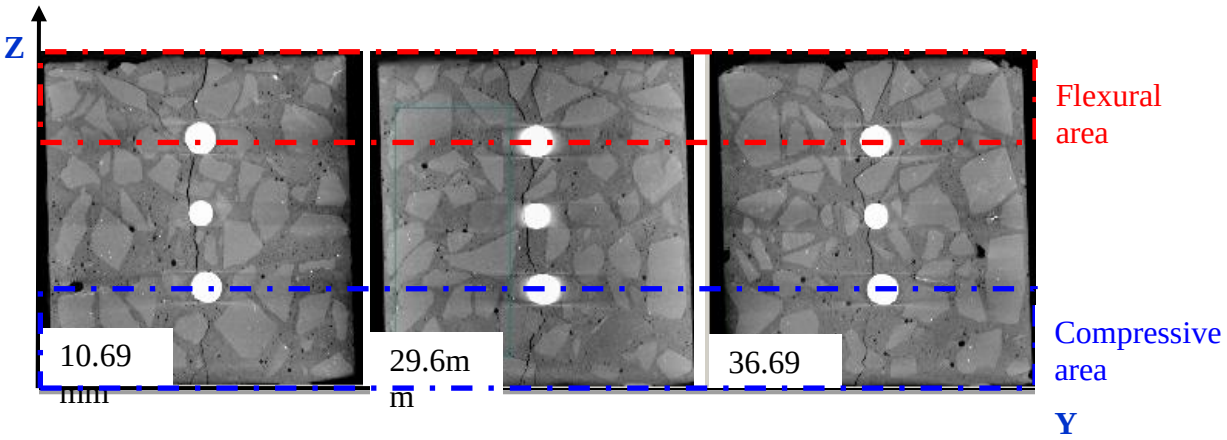

Figure 14. 2D images of YZ plane of reinforced concrete

So, the penetration time for oxygen and chloride ions to reach the surface of the steel bar in the Z direction is shorter than that in the Y direction. As such, the surface of the steel bar in the Y direction did not corrode. Further, the width and density of crack in flexural zone are more than that in the compressive zone. That is, the damage degree of cracked reinforced concrete at the tension zone is higher than that of the compressive zone. 26-year-old corroded RC beam from Zhu [25] also showed

that corrosion cracks were more developed in the tensile surface, both in frequency and width. The constant potential acceleration test did not affect the damage rule of reinforced concrete after cracking, and it is a better reflection of the influence of bending load on the damage degree of reinforced concrete after corrosion cracking.

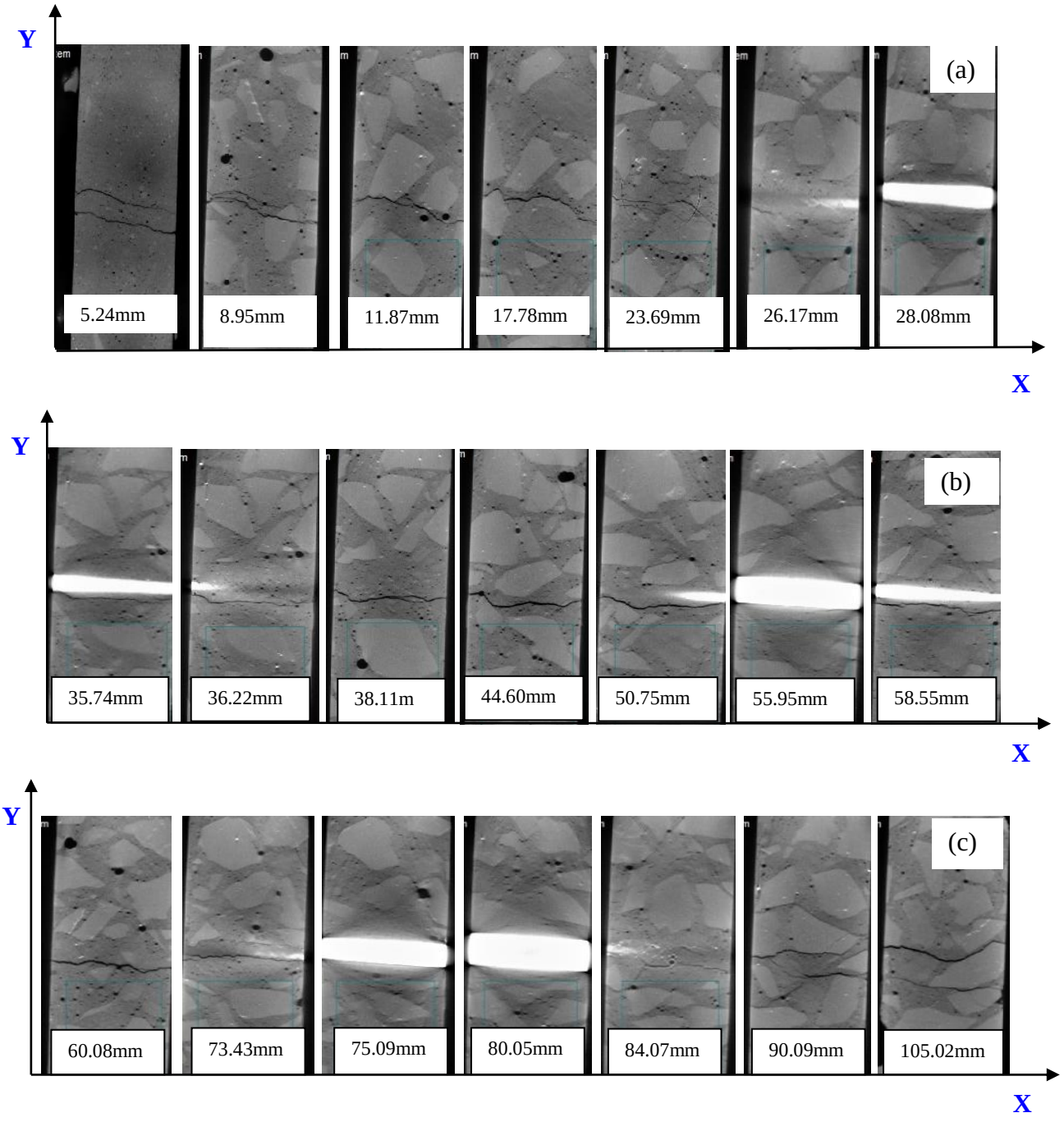

Figure 15. 2D images of XY plane of reinforced concrete.(a) from flexural area to tension steel bar,(b) from tension steel bar to stainless bar, (c) form stainless bar to compressive area

Fig.15 shows the images of one concrete specimen XY plane from the Z direction. In the flexural zone (5.24mm to 26.17mmfrom the concrete surface), there are two 0.8 mm wide cracks on

the surface of the specimen. Fig.15 (a) shows the crack width decreases to 0.1mm and the number of cracks reduces to one on the surface of the tension steel bar (i.e. 28.08 mm from the concrete surface). From the tension steel bar to the stainless bar and to the compression steel bar (i.e. from35.74mm to 50.75mm to 73.43mm), there is a thick crack in this zone, as shown in Figs.15(b) and15(c). The compressive zone is 80.05mm to 105.02mm from the concrete surface. The crack width increases gradually from the compression steel bar to the concrete surface. Therefore, when the reinforced concrete under the bending load was corroded in the constant potential acceleration method, the corrosive crack was not only observed in the flexural zone and the compressive zone, but also found in the zone between the steel bar and the stainless bar.

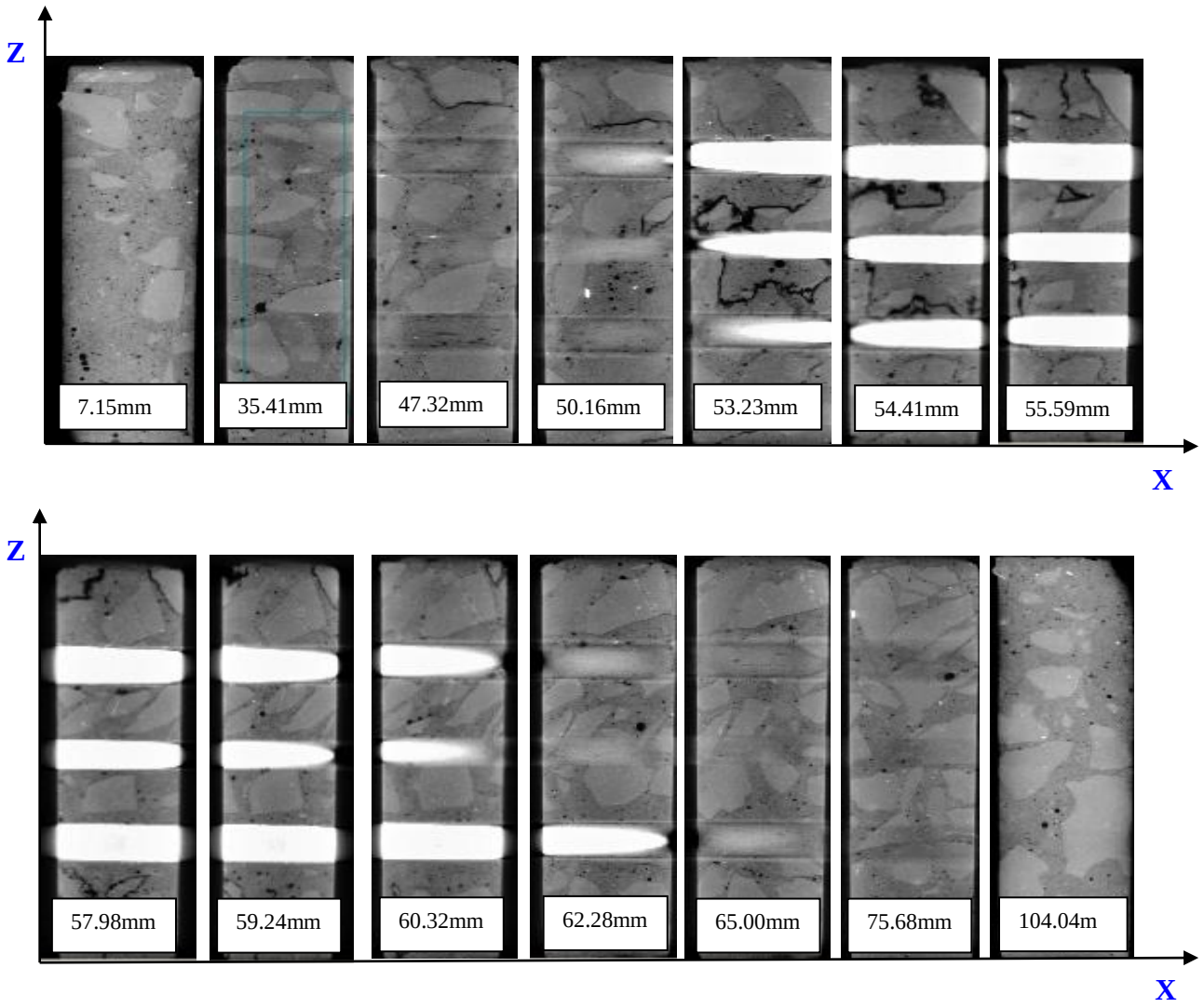

Figure 16. 2D images of XZ plane of reinforced concrete

Fig.16 shows the images of a concrete specimen on the XZ plane from the Y direction. In the flexural zone from the top of steel bar to the concrete surface, the crack propagates along the tension steel bar and expands to the concrete surface. At the concrete depth of 53.23mm, the crack can be observed in the zone from the tension steel bar to the stainless steel bar and to the compression steel

bar, and gradually found in the compressive zone. The corrosive crack primarily propagates along the steel bar in the longitudinal direction, and the transverse crack is less than 3 mm from the edge of the steel bar. It is apparent that under the constant potential test, the cracks in the concrete caused by the steel bar corrosion did not only propagate in the direction of concrete cover, but also towards the inside of the concrete between the steel bars. On the other hand, in real-life marine environment, the corrosion crack in reinforced concrete is primarily in the zone between the outside of the steel bar and the concrete surface[35].

In summary, the constant potential causes the chloride ion to penetrate into the surface of steel bar in a shorter period of time and reaches the critical concentration for steel bar corrosion earlier. As such, it is difficult to reflect the effect of real-life marine zones and loads on the penetration of chloride ion into concrete. Further, the crack in concrete induced by the constant potential acceleration method with embedded auxiliary stainless rebar electrode propagates in both the horizontal and vertical directions from the steel bar, which is inconsistent with the cracks in real-life structures in marine environment. Therefore, the constant potential acceleration method with embedded auxiliary stainless rebar electrode is not appropriate as an accelerated corrosion system for the study of corrosion process in reinforced concrete in marine environments.

4. CONCLUSIONS

The bending load causes the corrosion rate of steel bar in the flexural zone of concrete to accelerate, and the trend is only apparent with increasing load and after the concrete was cracked.

Corrosive crack primarily propagates along the steel bar in the longitudinal direction, and the transverse crack is less than 3 mm from the edge of the steel bar. The corrosive crack originates from the top and bottom of a deformed steel bar in the flexural and compressive zones of a concrete specimen, and then expands throughout the specimen along the middle line. The width and density of cracks in the flexural zone are more than those in the compressive zone.

The constant potential accelerated corrosion test with embedded stainless rebar electrode changes the corrosive crack direction and speed up chloride ion penetration velocity, which is different from those in real-life situation. What we recommended is to connect the reinforced bar with the positive terminal of a power supply and connect a stainless rebar or plate with the negative electrode as the reinforced concrete system was placed in the corrosion solution.

ACKNOWLEDGMENTS
This work is a part of a series of projects financially supported by the Chinese National Natural Science Foundation (NSF) Grant No. 51378269 and No.51420105015, and the Chinese National 973 project Grant No. 2015CB655100. Besides, this work is also supported by Chinese Railway Foundation Grant No. 2014G004-F.The leading author is sponsored by Shandong Province Government for his academic visit at University College London. All these are gratefully appreciated.

References

1. M.V. Biezma and J.R. San Cristobal, *Corros. Eng. Sci. Technol*., 40 (2005) 344.

2. B.R. Hou, W.H. Li and Z.Q. Jin, *Corrosion and repair reinforcement technology of reinforced concrete*, Beijing: Science press, 2012:5.
3. M.K. Moradllo, M. Shekarchi and M. Hoseini, *Constr. Build. Mater*., 30 (2012) 198.
4. T. Cheewaket, C.Jaturapitakkul and W.Chalee, *Constr. Build. Mater*., 37(2012) 693.
5. W.Chalee, P.Ausapanit and C. Jaturapitakkul, Mater. Des., 31(2010)1242.
6. J.G.Dai, Y.Akira and F.H.Wittmann, Cement Concrete Comp.,32(2010) 101.
7. M. Zhang, G. Ye and K. Breuge, *Mech. Res. Commun.*, 58 (2014) 64.
8. M. Ramli, W. H. Kwan and N. F. Abas, *Constr. Build. Mater*., 38 (2013) 554.
9. W.Xue, L. Zhang and Y.G. Xiong, *Procedia. Eng.*, 27(2012)1635.
10. A.Costa and J.Appleton, *Cement Concrete Comp.*,24(2002)169.
11. G.R.Meira, C.Andrade and C. Alonso, *Cement Concrete Comp*., 32 (2010)427.
12. A.Alhozaimy, R. R.Hussain and R.Al-Zaid, Constr. *Build Mater.*,28(2012)670.
13. R.Veraa, M.Villarroel and A.M.Carvajal, *Mater. Chem. Phys.*,114 (2009)467.
14. Z.Q.Jin, S.Gao, X.Zhao and L.Yang, *Int. J. Electrochem. Sci.*, 10(2015)625-636.
15. H.Fan, *Xi'an University of architecture and technology,* (2009) 35.
16. M.F.Lei, L.M.Peng and C.H.Shi, *Tunn. Undergr. Sp. Tech.*, 42 (2014) 15.
17. M.T.Bassuon and M.L.Nehdi, *Cement Concrete Res*., 39 (2009) 206.
18. S.J.Jaffer and C.M.Hansson, *Cement Concrete Res*., 39 (2009)116.
19. C.Q.Fang, K.Gylltoft, K Lundgren and M. Plos, *Cement Concrete Res*., 36(2006) 548.
20. L.Hariche, Y.Ballim, M.Bouhicha and S.Kenai, *Cement Concrete Comp*., 34 (2012) 1202.
21. Y.G. Du, M. Cullen, C. K. Li, *Constr. Build Mater*., 39 (2013) 148.
22. Odd E. Gjørv, *Durability design of concrete structures in severe environments*, (2009)15.
23. L.Abosrra, A.F. Ashour and M.Youseffi, *Constr. Build Mater*., 25 (2011) 3915.
24. M. M. Kashani, A. J. Crewe and N. A. Alexander, *Corros. Sci.*, 73 (2013) 208.
25. W.J.Zhu and R.Francois, *Constr. Build Mater*., 51 (2014) 461.
26. G.Malumbela, P.Moya and M.Alexander, *Constr. Build Mater.*, 23 (2009) 3346.
27. G.Malumbela, M.Alexander and P.Moya, *Constr. Build Mater*., 24 (2010) 17.
28. Y.X. Zhao, Y.Y. Wu and W.L. Jin, *Corros. Sci.*, 66 (2013)160-168.
29. G.Duffó, N.Gaillard and M.Mariscotti, *Cement Concrete Res.*, 74 (2015) 1.
30. E.N.Landis, E.N.Nagy and D. T.Kean, *J. Eng. Mech*., 70 (2003) 911.
31. S.R.Stock, N.K.Naik and A.P.Wilkinson, *Cement Concrete Res.*, 32(2002) 1673.
32. J.D. HAN, G.H. PAN and W. SUN, *J. Chin. Ceram. Soc*., 39 (2011) 75.
33. L. Chung, J.H.J. Kim and S.T. Yi, *Cement Concrete Comp*., 30 (2008) 603.
34. Raja Rizwan Hussain, *Cement Concrete Comp*., 33 (2011) 154.
35. Y.Yuan, Y.Ji, *Constr. Build Mater.*, 23 (2009) 2461.